Thermal and structural analysis of 4,5,6-trimethoxyisatin

Ana M.F. Oliveira-Campos[a]*, Lígia M. Rodrigues[a], Carla S. Francisco[a], Maria Jovita Oliveira[b], M. Manuela Silva[a], Michael J. Smith[a], Filipe A. Almeida Paz[c]

[a]*Centro de Química, Universidade do Minho, Campus de Gualtar, 4710-452 Braga, Portugal*

[b]*Instituto de Polímeros e Compósitos, Departamento de Engenharia de Polímeros, Universidade do Minho 4800-058 Guimarães, Portugal*

[c] *Universidade de Aveiro, CICECO, Departamento de Química, Campus Universitário de Santiago, 3810-193 Aveiro, Portugal.*

Abstract

4,5,6-Trimethoxyisatin was crystallized from water to give dark red needles that were characterized by NMR and IR spectroscopy, differential scanning calorimetry (DSC), thermogravimetric analysis (TGA), single-crystal X-ray diffraction (XRD) and hot-stage microscopy.

Keywords: Isatin; DSC; TGA; Hot-stage microscopy; Single-crystal X-ray diffraction (XRD)

1. Introduction

In the course of our study of indole alkaloids [1] and their precursors an unexpected melting behavior of purified crystals of 4,5,6-trimethoxyisatin [2] (Figure 1) attracted our attention. The observed anomaly consisted of an apparent transformation of the aspect of crystals during the melting process. This led us to explore the thermal and structural behavior in more detail. The compound was synthesized as described in the literature [2], characterized by the usual methods and was recrystallized from water to yield red needles. These crystals were studied using TGA and DSC. The complementary technique of hot-stage microscopy was also applied. Crystals were further studied using single-crystal X-ray diffraction.

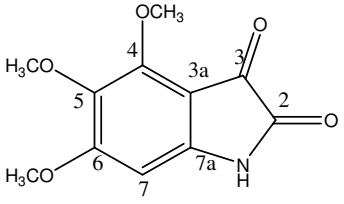

Figure 1 - Structure and atom numbering of 4,5,6-trimethoxyisatin

2. Experimental

2.1. NMR

^{1}H NMR spectrum was recorded at 300MHz and the ^{13}C NMR spectrum was determined at 75.4 MHz using a Varian Unity Plus Spectrometer. Double resonance, heteronuclear multiple quantum coherence (HMQC) and heteronuclear multiple bond correlation (HMBC) experiments were carried out for complete assignment of proton and carbon signals in the NMR spectrum. IR spectrum was registered on a Perkin Elmer FTIR-1600.

IV(Nujol mull), ν: 3313, 1759, 1692, 1623 cm^{-1}. ^{1}H NMR (DMSO-d_6, 300 MHz): δ 10.91 (s,1H, NH), 6.24 (s, 1H, H-7), 4.01 (s, 3H, 4-OMe), 3.89 (s, 3H, 6-OMe), 3.61 (s, 3H, 5-OMe). ^{13}C NMR (DMSO-d_6, 300 MHz): δ 178.73 (C-3), 162.55 (C-6), 160.46 (C-2), 152.93 (C-4), 148.94 (C-7a), 135.38 (C-5), 102.70 (C-3a), 91.88 (C-7), 61.63 (4-OMe), 61.02 (5-OMe), 56.83 (6-OMe).

2.2. Single-Crystal X-ray Diffraction

A suitable single-crystal of 4,5,6-trimethoxyisatin was manually harvested from the crystallization vial and was mounted on a Hampton Research CryoLoop with the aid of a Stemi 2000 stereomicroscope equipped with Carl Zeiss lenses and using FOMBLIN Y perfluoropolyether vacuum oil (LVAC 25/6) purchased from Aldrich [3]. Data were collected at 150(2) K on a Bruker X8 Kappa APEX II charge-coupled device (CCD) area-detector diffractometer (Mo K_α graphite-monochromated radiation, λ = 0.71073 Å) controlled by APEX2 software [4]. The equipment used to characterize samples included an Oxford Cryosystems Series 700 cryostream monitored remotely using the Cryopad [5] software interface. Images were processed using the software package SAINT+ [6] and data were corrected for absorption by the multi-scan semi-empirical method implemented in SADABS [7].

2.3. Differential scanning calorimetry (DSC)

Differential scanning calorimetry measurements were performed using a Mettler DSC 821e, calibrated with indium to ensure the accuracy of the calorimetric scale. Weighed samples (0.5–1.5 mg) were characterized in sealed 40 μL aluminium cans with perforated lids and subjected to thermal analysis under a flowing argon atmosphere (35 mL min^{-1}). In the preliminary phase of the study a variety of experimental conditions were applied to optimize heating and cooling rates for observation of the thermal events. Selected samples were heated from room temperature to 225 ^{o}C at a rate of 10 ^{o}C min^{-1}. These samples were subsequently

cooled to −60 ^{o}C at a rate of 5 ^{o}C min^{-1}. A second heating program, between −60 ^{o}C and 225 ^{o}C at a rate of 10 ^{o}C min^{-1} was then applied.

2.4. Thermogravimetric studies (TG)

Samples for thermogravimetric analysis were placed inside open platinum crucibles and studied using a Rheometric Scientific TG1000 thermobalance operating under a flowing argon atmosphere (28 mL min^{-1}). A heating rate of 10 ºC min^{-1} was used and all samples were studied between 30 and 400 ºC.

2.5. Hot stage microscopy studies

A small number of dry crystals were mounted between a glass slide and a cover slip, placed on a Mettler FP 82 hot stage and observed with a polarized light Olympus BH2 microscope equipped with a digital camera. The calibration of the temperature scale was carried out in accordance with the manufacturer's instructions. The samples were heated to complete melting at a rate of 10 ºC min^{-1}, fast cooled to room temperature at about 40 ºC min^{-1} and re-heated again at 10 ºC min^{-1}.

3. Results and discussion

3.1. Crystal Structure Description

The structure was solved in the centro-symmetric $P2_1/c$ space group using the direct methods algorithm implemented in SHELXS-97 [8,9], which allowed the immediate location of the vast majority of the atoms belonging to the crystallographically independent molecule. All remaining non-hydrogen atoms were located from difference Fourier maps calculated from successive full-matrix least squares refinement cycles on F^2 using SHELXL-97 [9,10]. All non-hydrogen atoms were successfully refined using anisotropic displacement parameters.

Even though all hydrogen atoms bound to carbon and nitrogen were clearly visible in difference Fourier maps, these have been located at their idealized positions using appropriate *HFIX* instructions in SHELXL (*43* for the aromatic and the N–H moiety, and *137* for the terminal methyl groups) and included in subsequent refinement cycles in riding-motion approximation with isotropic thermal displacements parameters (U_{iso}) fixed at 1.2 (for the former families of hydrogen atoms) or 1.5 (for the methyl moieties) times U_{eq} of the carbon atom to which they are attached. The final difference Fourier map synthesis showed the highest peak (0.429 eÅ^{-3}) and deepest hole (-0.261 e Å^{-3}) located at 0.65 Å from C(3) and 1.17 Å from C(1), respectively.

Information concerning crystallographic data collection and structure refinement details is summarized in Table 1.

Table 1 - Crystal and structure refinement data for 4,5,6-trimethoxyisatin.

Formula	$C_{11}H_{11}NO_5$
Formula weight	237.21
Crystal system	Monoclinic
Space group	$P2_1/c$
a/Å	3.8384(9)
b/Å	24.573(5)
c/Å	11.015(3)
α/º	90
β/º	97.928(14)
γ/º	90
Volume/Å^3	1029.0(4)
Z	4
Z'	2
D_c/g cm^{-3}	1.531
μ(Mo-Kα)/mm^{-1}	0.123
Crystal size/mm	0.40×0.10×0.08
Crystal type	Red needles
θ range	3.74 to 33.14
Index ranges	$-5 \le h \le 5$
	$-37 \le k \le 37$
	$-16 \le l \le 16$
Reflections collected	26099
Independent reflections	3822 (R_{int} = 0.0500)
Completeness to θ = 33.14º	98.1%
Final *R* indices [I>2σ(I)][a,b]	*R*1 = 0.0474
	*wR*2 = 0.1227
Final *R* indices (all data)[a,b]	*R*1 = 0.0814
	*wR*2 = 0.1396
Weighting scheme[c]	*m* = 0.0729
	n = 0.0933
Largest diff. peak and hole	0.429 and -0.261 eÅ^{-3}

[a] $R1 = \sum \left| |F_o| - |F_c| \right| / \sum |F_o|$

[b] $wR2 = \sqrt{\sum \left[w\left(F_o^2 - F_c^2\right)^2 \right] / \sum \left[w\left(F_o^2\right)^2 \right]}$

[c] $w = 1/\left[\sigma^2\left(F_o^2\right) + (mP)^2 + nP \right]$ where $P = \left(F_o^2 + 2F_c^2\right)/3$

The derivative 4,5,6-trimethoxyisatin crystallizes in a manner similar to that observed for the parent and previously-characterized isatin molecule [11] at 150 K in the centro-symmetric $P2_1/c$ space group with the asymmetric unit comprising a single molecular unit as depicted in Figure 2. It is interesting to note that the three methoxy substituent groups impose a considerable steric hindrance to the orderly packing in the solid state in 4,5,6-trimethoxyisatin, ultimately leading to an overall deformation of the molecule. Indeed, while in isatin the two conjugated rings are almost co-planar (with an average dihedral angle of only about 0.3º) [11], in 4,5,6-trimethoxyisatin the plane of the benzene ring is considerably tilted (by *ca.* 5.6º) from that containing the heterocyclic moiety.

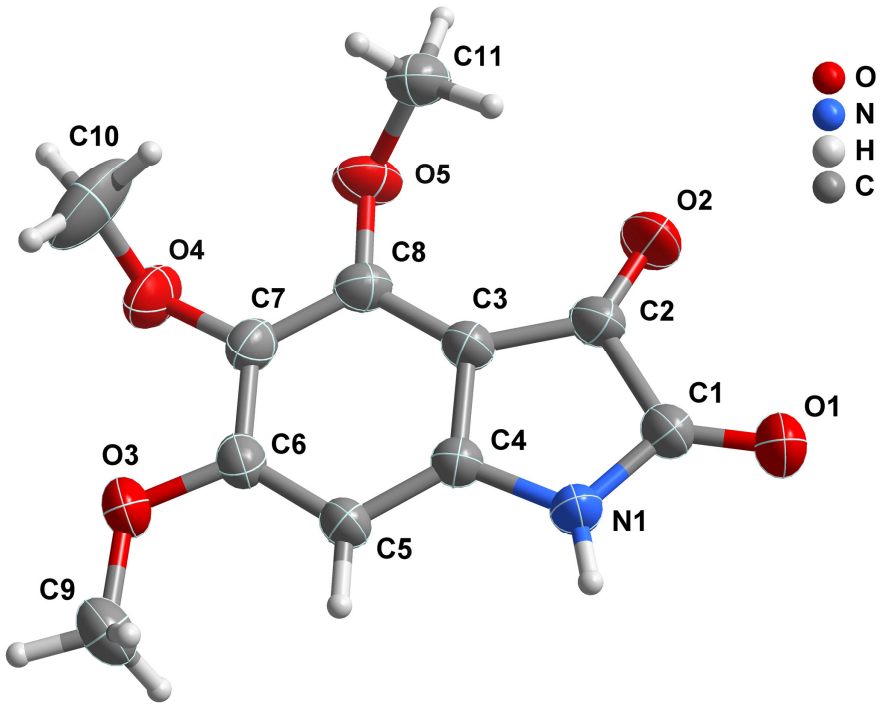

Figure 2 – Schematic representation of the molecular unit of 4,5,6-trimethoxyisatin. Non-hydrogen atoms are represented as thermal ellipsoids drawn at the 80% probability level and showing the labelling scheme. Hydrogen atoms are drawn as small spheres with arbitrary radii.

Individual molecules of 4,5,6-trimethoxyisatin interact in the solid state via strong and highly directional N–H···O hydrogen bonds [N1–H1···O2^{i}, d(D···A) = 2.7922(15) Å with ∠(DHA) = 147º; symmetry code: (i) *-1+x*, *½-y*, *-½+z*] connecting the N–H moiety of one molecule to the C2–O2 carbonyl of the neighbouring one (Figure 3). This leads to a

supramolecular chain of molecules distributed in a typical zigzag fashion along the [25 0 116] direction which minimizes steric repulsion between the substituent groups. The strength of these hydrogen bonding interactions leads to a lengthening of the C=O bond distance to 1.2175(15) Å which is, as expected, markedly longer than those typically observed in related isatin molecule derivatives: from a systematic search in the Cambridge Structural Database (CSD, Version 5.30 with one update of November 2008), 16 hits were found with the C=O moieties registering bond distances ranging from 1.173 to 1.218 Å (median 1.208 Å). It is also noteworthy that this supramolecular arrangement of molecules is markedly different from that typically observed for isatin where neighbouring molecules interact via $R_2^2(8)$ graph set motifs (involving the N–H and C=O moieties) [12] leading to discrete dimeric entities. The crystal packing for both isatin and 4,5,6-trimethoxyisatin (Figure 4) is essentially mediated by a series of weak C–H···O hydrogen bonds and offset π-π stacking (not shown) involving in the former compound the supramolecular dimers and in the latter the aforementioned one-dimensional chain. In addition, the rotation of the three methoxy substituent groups also seems to occur in such a way that maximizes the number of weak C–H···O interactions.

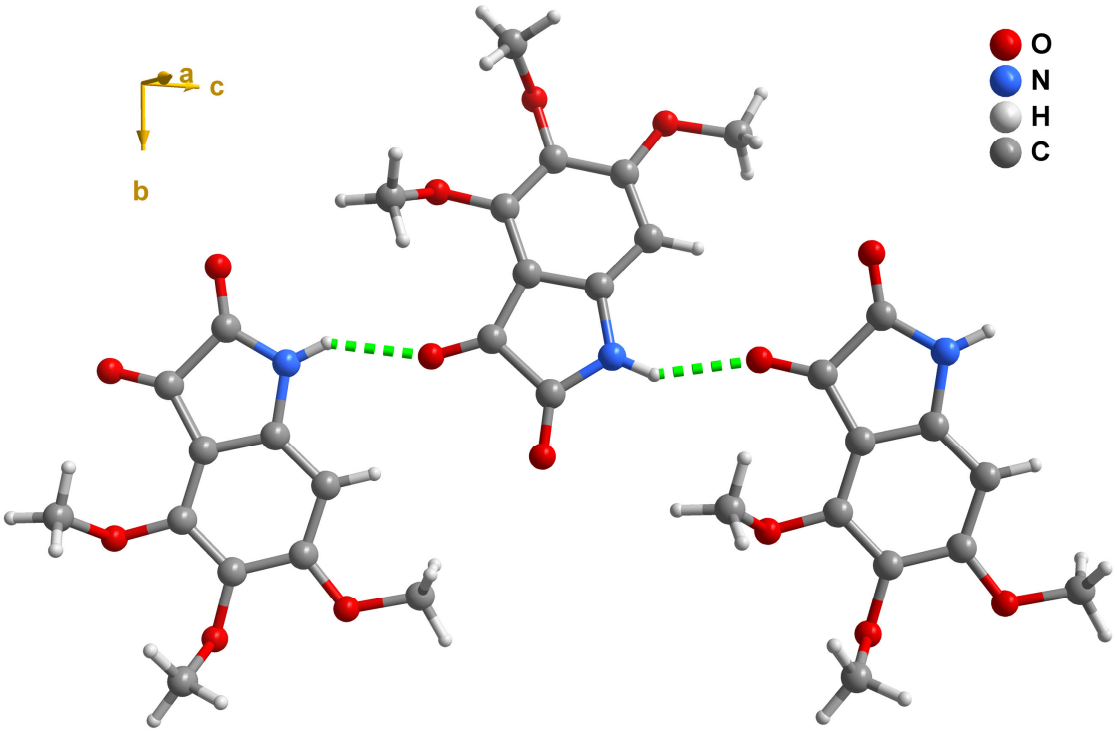

Figure 3 – One-dimensional supramolecular tape of 4,5,6-trimethoxyisatin molecules running parallel to the [25 0 116] direction of the unit cell and assembled by the N–H···O hydrogen bonds connecting adjacent molecular units.

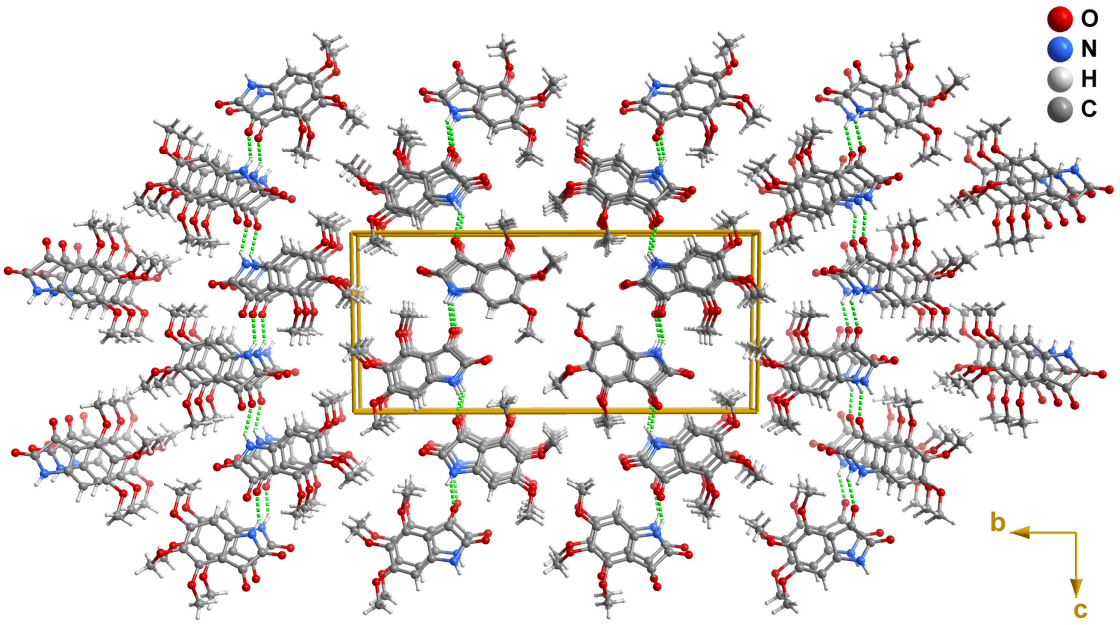

Figure 4 – Crystal packing of 4,5,6-trimethoxyisatin viewed in perspective along the [100] direction of the unit cell.

3.2. Variable temperature X-ray diffraction

The X-ray diffraction pattern of a sample of 4,5,6-trimethoxyisatin was recorded as a function of temperature and the observed evolution with temperature is illustrated in Figure 5. The results provide further support for the existence of structural changes between 150 and 200ºC.

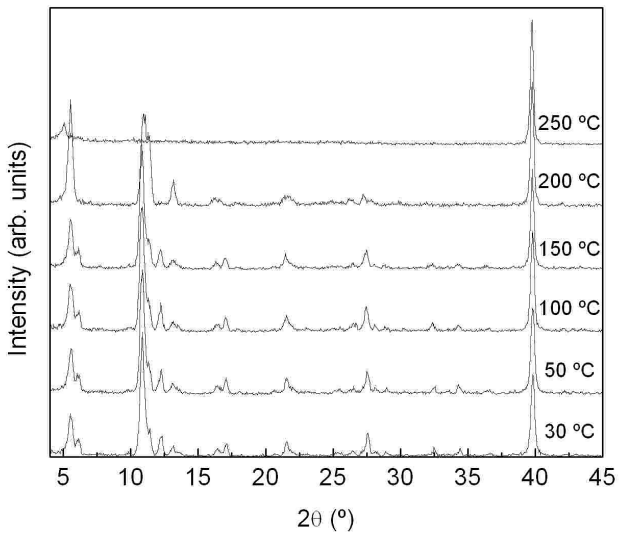

Figure 5 – X-ray diffraction of 4,5,6-trimethoxyisatin as a function of temperature.

3.3. Hot stage microscopy studies

During the first heating cycle of the dye crystals noteworthy changes took place in the visual aspect of the sample at temperatures of about 172 ºC and 215-216 ºC (Figure 6). This latter transformation occurred in the peripheral region of the newly-formed liquid phase and involved the appearance of small acicular crystals in the region surrounding the liquid phase. During cooling of the sample, crystallization of the liquid phase occurred and this process was accompanied by the formation of a crown of acicular crystals. When the sample was subjected to a second heating cycle the material previously recrystallized from the liquid phase melted again at 212 ºC, however the acicular crystals surrounding this region did not melt, even when heated up to 274 ºC.

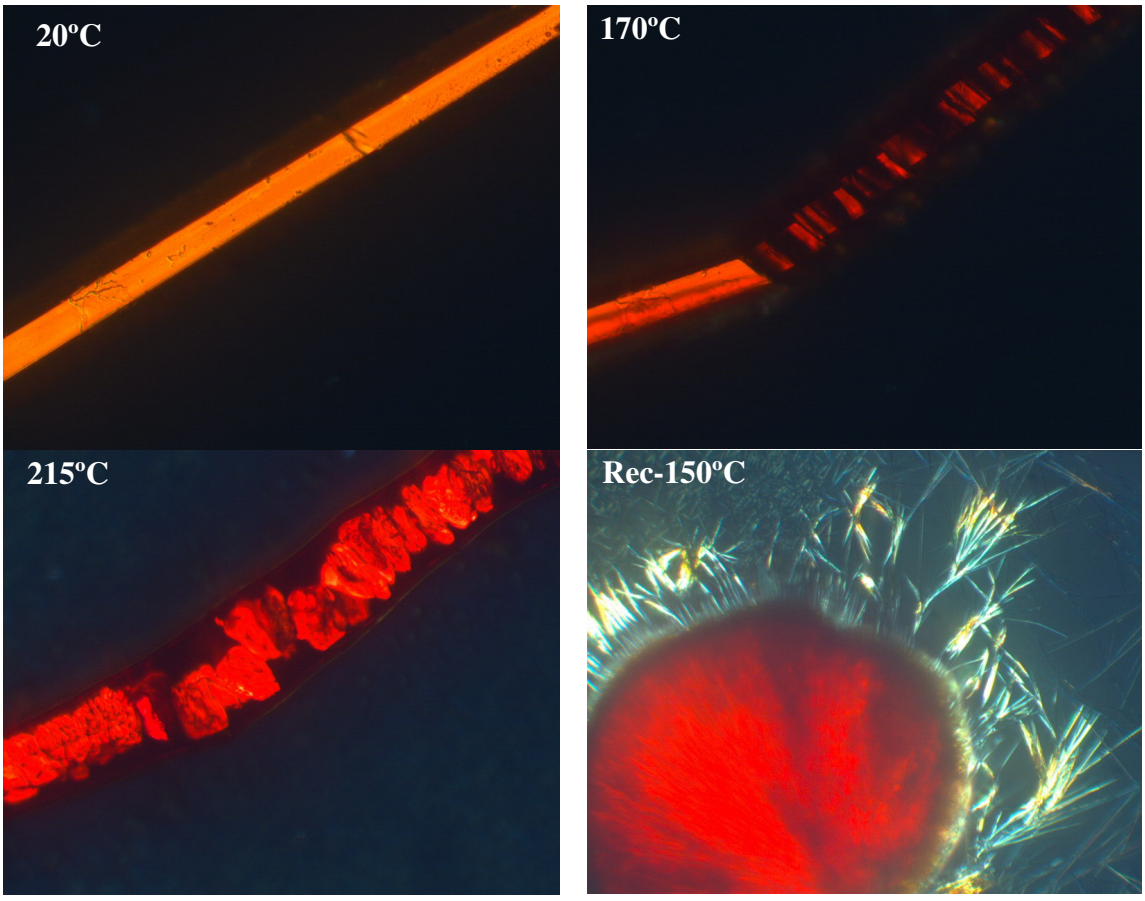

Figure 6- Photomicrographs of 4,5,6-trimethoxyisatin at several temperatures

The crystallographic data show hydrogen bonding between adjacent molecules leading to the formation of a supramolecular chain. The thermal event beginning at 172 ºC may be caused by partial change or rearrangement of the crystalline network, possibly due to destruction of

the π-π stacking. At higher temperatures the melting continues as the destruction of N–H···O hydrogen bonds proceed.

In the ^{1}H NMR (Nuclear Magnetic Resonance) spectrum, in DMSO solution, the high chemical shift of the NH signal (10.91 ppm), suggests that this proton is involved in a hydrogen bond.

3.4. DSC and TGA studies

The results obtained from DSC characterization may be correlated with those observed using hot-stage microscopy. The thermogram of this sample is dominated by an intense well-defined narrow endothermic peak with an extrapolated onset at about 210 ºC (Figure 7, 2nd heating).

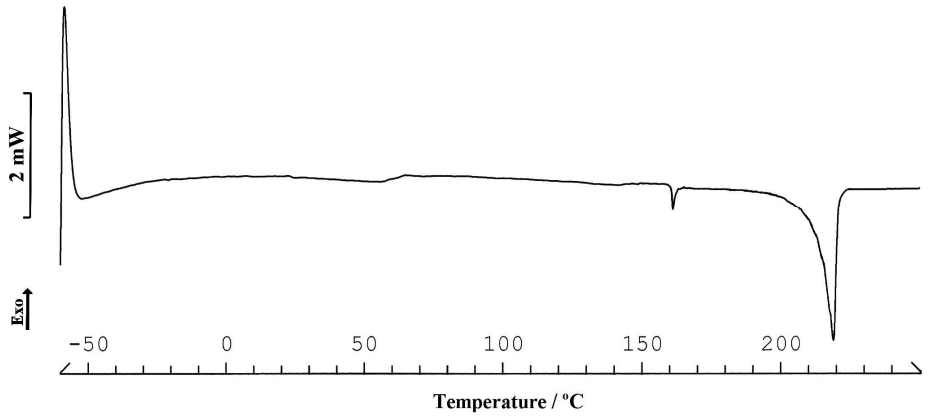

Figure 7- DSC curve: second heating run

TGA measurements confirmed that weight loss began between 190 and 205 ºC, supporting the suggestion that over this temperature range thermal degradation of the sample begins and progresses until close to 230 ºC (Figure 8).

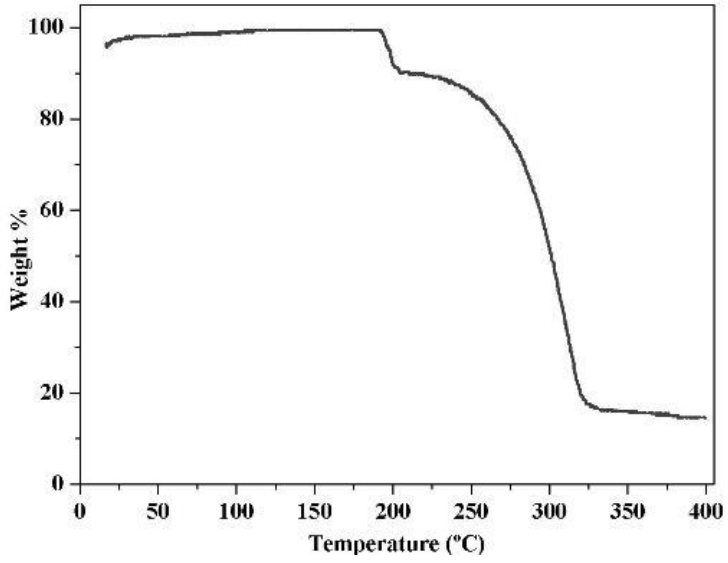

Figure 8- Thermogravimetry curve

The results of the thermogravimetric study suggest that the degradation of this sample occurs in two distinct phases, probably with rearrangement of the molecular structure and the loss of a small molecule (lost of CO [11]). The first heating experiment was stopped at about 210 ºC, at the onset of degradation. The sample was cooled to room temperature at 10 ºC min^{-1}. At about 180 ºC a sharp exothermic crystallization peak, was observed. During the second heating a weak endothermic event was observed at 160 ºC. This may be associated with the phase change observed by hot-stage microscopy at about 170 ºC (Figure 6).

A rather weak and disperse thermal event was also registered in the thermogram with an onset of 84 ºC, however attribution of this event to an identifiable thermal process has not been possible. There is no discernible weight loss associated with this exotherm and as it appears in both first and second heating curves it seems unlikely that it is caused by evolution of residual solvent from the sample.

4. Conclusions

In this study 4,5,6-trimethoxyisatin was characterized by structural and thermal techniques to determine the nature of the anomalous melting behaviour. The results of this study suggest that crystals of this substance undergo a phase transition with an onset at about 160-175 ºC. Thermal degradation of the sample occurs in a two-stage process at temperatures close to 200 ºC.

5. Supplementary material

Crystallographic data (excluding structure factors) have been deposited with the Cambridge Crystallographic Data Centre as supplementary publication No. CCDC-695191. Copies of the data can be obtained free of charge on application to CCDC, 12 Union Road, Cambridge CB2 2EZ, U.K. FAX: (+44) 1223 336033. E-mail: deposit@ccdc.cam.ac.uk.

Acknowledgements

The authors are pleased to thank *Fundação para a Ciência e a Tecnologia* (FCT) (POCTI-SFA-3-686) and FEDER (Portugal) for financial support and specific funding towards the purchase of the single-crystal X-ray diffractometer.

References

[1] M.J.E. Hewlins, A.H. Jackson, A.M. Oliveira-Campos and P.V.R. Shannon, J. Chem. Soc. Perkin Trans. (1981) 2906.

[2] F. Benington, R.D. Morin, and Leland C. Clark, J. Org. Chem. 20 (1955) 1454.

[3] T. Kottke, D. Stalke, J. App. Cryst. 26 (1993) 615.

[4] APEX2, Data Collection Software Version 2.1-RC13, Bruker AXS, Delft, The Netherlands, 2006.

[5] Cryopad, Remote monitoring and control, Version 1.451, Oxford Cryosystems, Oxford, United Kingdom, 2006.

[6] SAINT+, Data Integration Engine v. 7.23a©, Bruker AXS, Madison, Wisconsin, USA, 1997-2005.

[7] G.M. Sheldrick, SADABS v.2.01, Bruker/Siemens Area Detector Absorption Correction Program, Bruker AXS, Madison, Wisconsin, USA, 1998.

[8] G.M. Sheldrick, SHELXS-97, Program for Crystal Structure Solution, University of Göttingen, 1997.

[9] G.M. Sheldrick, Acta Cryst. A 64 (2008) 112.

[10] G.M. Sheldrick, SHELXL-97, Program for Crystal Structure Refinement, University of Göttingen, 1997.

[11] H.X. Wei, Z. Chun, S. Ham, J.M. White, D.M. Birney, Org. Lett. 6 (2004) 4289.

[12] J. Bernstein, R.E. Davis, L. Shimoni, N.L. Chang, Angew. Chem. Int. Edit. Engl. 34 (1995) 1555.